Photonic crystal based microscale flow cytometry

Justin Stewart[1] and Anna Pyayt[1,*]

[1]*IBIS Lab, Department of Chemical and Biomedical Engineering, University of South Florida, 4202 E. Fowler Avenue, Tampa, F.L. 33620, USA*
[*]*pyayt@usf.com*

Abstract: Here we propose a new design of an on-chip micro-flow cytometry based on photonic crystals. When individual cells flow tangential to the crystal surface, the transmission of the light through the photonic crystal changes depending on the presence or absence of the cells and their size and shape. This system was modeled using OptiFDTD, where transmission spectra were extracted. Initially, the potential for cell counting has been demonstrated. Then, for cells with differing shape a direct relation between signal distribution and cell shape has been found.

OCIS codes: (170.0170) Medical optics and biotechnology; (120.3890) Medical optics instrumentation.

References and links

1. O. D. Laerum and T. Farsund, "Clinical Application of Flow Cytometry: a review," Cytometry **2**(1), 1–13 (1981).
2. P. Mullaney and J. Jett, "Flow Cytometry: An Overview," Lasers Biol. Med. **34**, 179–193 (1980).
3. R. Chang, "Flow cytometry's new scalability," BioOptics World, (2008). *http://www.bioopticsworld.com/articles/print/volume-1/issue-4/features/feature-focus/flow-cytometryrsquos-new-scalability.html*
4. M. May, "Optical Diagnostics/Flow Cytometry: Advances in optical biodetection," BioOptics World, (2013). *http://www.bioopticsworld.com/articles/print/volume-6/issue-1/features/advances-in-optical-biodetection.html*
5. S. Seo, T. W. Su, D. K. Tseng, A. Erlinger, and A. Ozcan, "Lensfree holographic imaging for on-chip cytometry and diagnostics," Lab Chip **9**(6), 777–787 (2009).
6. D. A. Ateya, J. S. Erickson, P. B. Howell, Jr., L. R. Hilliard, J. P. Golden, and F. S. Ligler, "The good, the bad, and the tiny: a review of microflow cytometry," Anal. Bioanal. Chem. **391**(5), 1485–1498 (2008).
7. S. Y. Yang, K. Y. Lien, K. J. Huang, H. Y. Lei, and G. B. Lee, "Micro flow cytometry utilizing a magnetic bead-based immunoassay for rapid virus detection," Biosens. Bioelectron. **24**(4), 855–868 (2008).
8. H. T. Huang, T. R. Ger, Y. H. Lin, and Z. H. Wei, "Single cell detection using a magnetic zigzag nanowire biosensor," Lab Chip **13**(15), 3098–3104 (2013).
9. T. R. Ger, H. T. Huang, C. Y. Huang, and M. F. Lai, "Single cell detection using 3D magnetic rolled-up structures," Lab Chip **13**(21), 4225–4230 (2013).
10. S. C. Hur, H. T. Tse, and D. Di Carlo, "Sheathless inertial cell ordering for extreme throughput flow cytometry," Lab Chip **10**(3), 274–280 (2010).
11. G. Lee, C. Lin, and G. Chang, "Micro flow cytometers with buried SU-8/SOG optical waveguides," Sens. Actuators A Phys. **103**(1-2), 165–170 (2003).
12. A. L. Pyayt, D. A. Fattal, Zh. Li, and R. G. Beausoleil, "Nanoengineered optical resonance sensor for composite material refractive-index measurements," Appl. Opt. **48**(14), 2613–2618 (2009).
13. D. Fattal, M. Sigalas, A. L. Pyajt, Zh. Li, and R. G. Beausoleil, "Guided-mode resonance sensor with extended spatial sensitivity", Proc. SPIE **6640**, 66400M (2007).
14. N. Watkins, B. M. Venkatesan, M. Toner, W. Rodriguez, and R. Bashir, "A robust electrical microcytometer with 3-dimensional hydrofocusing," Lab Chip **9**(22), 3177–3184 (2009).
15. A. J. Chung, D. R. Gossett, and D. Di Carlo, "Three dimensional, Sheathless, and High-Throughput Microparticle Inertial Focusing Through Geometry-Induced Secondary Flows," Small **9**(5), 685–690 (2013).
16. X. Xuan, J. Zhu, and C. Church, "Particle focusing in microfluidic devices," Microfluid. Nanofluid. **9**(1), 1–16 (2010).
17. http://optiwave.com/category/products/component-design/optifdtd/
18. T. Bååk, "Silicon oxynitride; a material for GRIN optics," Appl. Opt. **21**(6), 1069–1072 (1982).
19. G. Ghosh, "Dispersion-equation coefficients for the refractive index and birefringence of calcite and quartz crystals," Opt. Commun. **163**(1-3), 95–102 (1999).

#207945 - $15.00 USD Received 10 Mar 2014; revised 17 Apr 2014; accepted 29 Apr 2014; published 20 May 2014

20. Y. L. Jin, J. Y. Chen, L. Xu, and P. N. Wang, "Refractive index measurement for biomaterial samples by total internal reflection," Phys. Med. Biol. **51**(20), N371–N379 (2006).
21. T. R. Gregory, "The Bigger the C-Value, the Larger the Cell: Genome Size and Red Blood Cell Size in Vertebrates," Blood Cells Mol. Dis. **27**(5), 830–843 (2001).
22. W. Jin, Y. Wang, N. Ren, M. Bu, X. Shang, Y. Xu, and Y. Chen, "Simulation of simultaneous measurement for red blood cell thickness and refractive index," Opt. Lasers Eng. **50**(2), 154–158 (2012).
23. V. Maltsev, A. Hoekstra, and M. Yurkin, "Optics of White Blood Cells: Optical Models, Simulations, and Experiments," in *Advanced Optical Flow Cytometry: Methods and Disease Diagnoses,* (Academic, 2011), pp. 63–93.

1. Introduction

Analytical methods for studying individual cells with high throughput have been critical for molecular biology, immunology and pathology. In addition, advancements in high throughput cell screening have greatly assisted in the discovery of new drugs. Among available techniques, flow cytometry has become the most widely used method for analyzing and characterizing cells [1]. Traditional flow cytometry units are complex systems which employ multiple lasers and sophisticated optical detectors designed primarily for cell counting, shape characterization, and multi-colored fluorescence analysis [2]. Despite having many benefits, these systems have significant limitations due to their large size, high prices and complex operation [3].

Today, the rising need for 'Point-of-Care' devices has led to an increased demand for more portable, and lower cost flow cytometers. However, benchtop units are still the smallest among commercially available flow cytometers, and they are heavy and not readily portable [3]. Ongoing research in miniaturizing flow cytometers into handheld devices has made significant progress over the past few years. Nonetheless, smaller devices have had to sacrifice many capabilities, including detection on multiple wavelengths [4]. Another promising method relies on digital processing of diffraction patterns of different cell types [5]. However, these diffraction pattern techniques are not performed with flowing fluids, therefore continuous cell differentiation cannot be achieved [5].

Advances in MEMS and microfluidics has provided an opportunity to reproduce the functionality of large scale flow cytometry units with high cell throughput at much smaller scale. The proposed micro-flow cytometers often incorporate some method of cell focusing in conjunction with optical, magnetic or electrical detection components, into a single device that can easily fit onto a chip [6]. Regardless, micro-flow cytometers have experienced difficulty in providing functions analogous to traditional flow cytometers due to either more complex detection methods or lower resolution optical detectors. Specifically, devices relying on magnetic detection suffer from increased complexity in sample preparation, as cells are not inherently magnetic. As a result, cells must be labeled with magnetic nanoparticles, before they can be detected [7–9]. Additionally, while demonstrating great promise in continuously counting cells, magnetic and electric-based micro-flow cytometers are unable to perform certain functions such as fluorescent studies for cellular expression. On the other hand, optics-based micro-flow cytometers struggle with low resolution. At the microscale, light diffracts at wide angles, and as a result there are significant losses between light sources and detectors. In order to overcome diffraction limitations, waveguides and optical detectors are often very large, to the point that these components are generally several cell diameters in width [10, 11]. Due to this, optical detection in micro-flow cytometry often experiences difficulty resolving individual cells within close proximity of each other, due to the optical component's high field of view [10, 11].

Here we propose a new method for optical detection in micro-flow cytometry using transmission spectra of a photonic crystal (Ph.C.). Traditionally, Ph.C.s have been used for refractive index-based sensing [12, 13]. Based on FDTD simulations, we demonstrate that by using more sophisticated spectrum analysis it is possible to design a Ph.C. micro-flow cytometer capable of achieving functionality similar to traditional flow cytometry units, however at a significantly smaller scale and potentially lower cost.

#207945 - $15.00 USD Received 10 Mar 2014; revised 17 Apr 2014; accepted 29 Apr 2014; published 20 May 2014

2. Device principles and simulation parameters

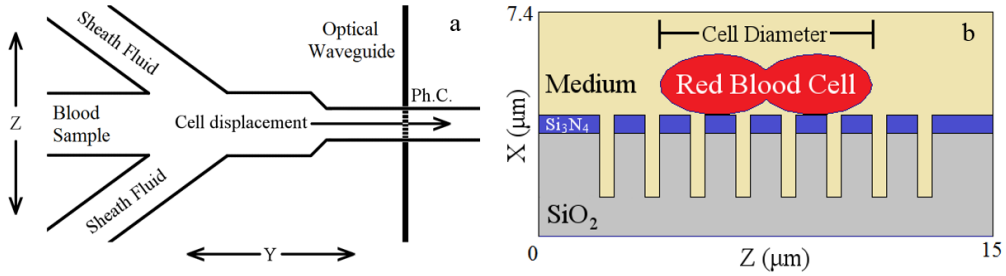

Fig. 1. (a) Theoretical layout of the device on chip where cell focusing is conducted on the left and optical detection using Ph.C. on the right. (b) Cross Sectional view of the Ph.C. Here the material in grey represents silicon dioxide, blue - silicon nitride core of the Ph.C., yellow - surrounding medium, and the red object is a red blood cell.

The theoretical design of the device is presented in Fig. 1. As with all micro-flow cytometers, a blood sample must first be spatially focused into a narrow stream of individual cells. Spatial focusing of cells can be achieved through many well-studied techniques such as hydrodynamic focusing with a sheath fluid, or through 'sheath-less' inertial focusing methods [14–16]. Regardless of the procedure used, these cells must be focused for the device to behave as desired. Studies on the vertical positioning of cells have demonstrated a capability to push cells extremely close to the surface of a microfluidic chamber using a sheath fluid [14]. With this in consideration, cells were modeled close to the surface to allow for greater interaction with the Ph.C. In Fig. 1(a), a schematic for the system with hydrodynamic focusing is shown. Once the cells have been properly aligned, the stream flows over the surface of a 1-D Ph.C. where individual cells will interfere with the transmission of light through the crystal. By studying changes in the transmission spectrum, information regarding the cells can be determined.

The device was designed and simulated in 2-D with OptiFDTD [17] to model the propagation of light through the photonic crystal. A general schematic of the Ph.C. cross section is represented above in Fig. 1(b). The Ph.C. consists of two materials, a 0.6 μm thick layer of silicon nitride (refractive index 2.03) shown in blue [18], and silicon dioxide (refractive index 1.54) shown gray [19], serving as a cladding. The design of the Ph.C. includes periodic slits patterned in the nitride layer 0.5 μm wide and 2.7 μm deep. Spacing of each slit was 1.5 μm from their center, with a total of eight slits over the entire Ph.C. The structure was then considered completely submerged in a liquid medium for analysis, shown in yellow (plasma with the refractive index 1.3515 [20]). The medium was allowed to fill the slits. Finally red blood cells (6-8 μm, refractive index 1.38 [21, 22]) were flown over the surface of the crystal. In order to model cell flow across the Ph.C. surface (displacement in y direction - δy) in a 2-D FDTD model (x and z directions), the geometry of cell cross-sections based on incremental displacement of the cell were calculated and simulated for each iteration, as the cell moved through the plane of study. The geometries of these 2-D cell cross sections were calculated under the assumption that blood cells may be approximated as biconcave discs, whose cross section is composed of overlapping ellipses as seen in Fig. 1(b). In addition, each blood cell was assumed to be perfectly symmetric around the center. Therefore, displacement only had to be calculated from the center (δy = 0 μm) to the edge of the cell (δy = R μm). Due to the symmetry assumption, results were reflected across the origin to visualize the effects of the entire cell movement through the observation plane. Furthermore, the refractive index of the surrounding media was assumed to be held constant for the duration of each simulation.

The transmission spectrum was calculated between 450 and 550 nm, and normalized with respect to the input light spectrum.

#207945 - $15.00 USD Received 10 Mar 2014; revised 17 Apr 2014; accepted 29 Apr 2014; published 20 May 2014

3. Results and discussions

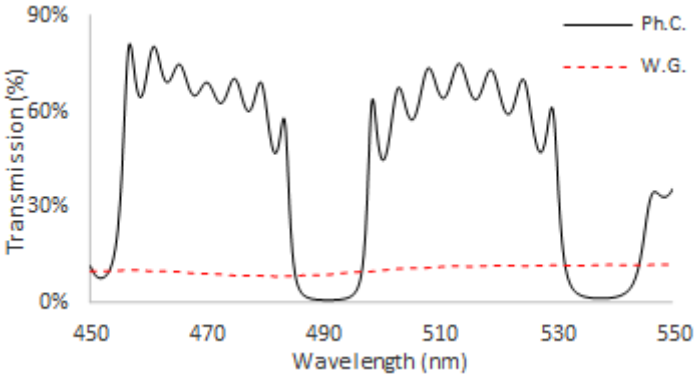

Fig. 2. Calculated transmission spectrum of the Ph.C. (black) as compared to a disrupted optical waveguide (red) of equal thickness.

In order to apply this micro-flow cytometer to plasma and whole blood analysis, the initial spectrum was calculated for the Ph.C device fully immersed in plasma (refractive index 1.3515) (Fig. 2). The band gaps and regions of high transmission can be clearly identified. Electric field distributions (Ey) are provided in Fig. 3 for two different wavelengths. At a wavelength of 490.0 nm, light is incapable of transmitting through the crystal, which corresponds to the bang gap region as seen in Fig. 2, while at a wavelength of 513.3 nm light is going through.

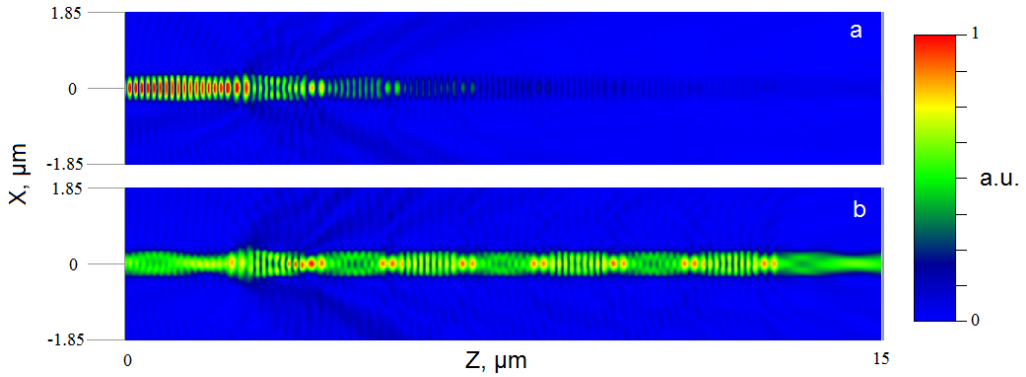

Fig. 3. Electric field (E_y) distribution through the Ph.C. immersed in plasma for the (a) Band gap wavelength 490.0 nm, and (b) Peak transmission wavelength 513.3 nm.

Different regions of Ph.C. spectra can be used for different applications – the same device may operate at multiple wavelengths, all of which provide comparable information and may be interchangeable if additional channels of detection (e.g. fluorescence) are needed. For example in Fig. 2, the wavelength region 455-485 nm may be used for counting and assessing cells as they flow past the device, while the second region shown (495-532 nm) may be used to perform fluorescent studies with dyes that emit light at those specific wavelengths. Once the size of the cell has been determined from the first region, a baseline transmission can be extrapolated for the entire spectrum based on the models of non-florescent cells. Any increase in transmission due to emission from fluorescent dyes in the second region may then be quantified for the expression study.

Additionally, in Fig. 2, transmission through the Ph.C. is compared to that of a "disrupted" optical waveguide, a component previously proposed for micro-flow cytometry devices [11]. This disrupted waveguide was simulated for the same materials and dimensions

#207945 - $15.00 USD Received 10 Mar 2014; revised 17 Apr 2014; accepted 29 Apr 2014; published 20 May 2014

as layers of the Ph.C. and it may be clearly seen that transmission in the Ph.C. is exceedingly greater than what is observed with the disrupted optical waveguide. In order to increase transmission the disrupted waveguide has to be significantly larger, but this would considerably decrease the resolution of the device, since it is inversely proportional to the dimensions of the optical components. Ideally, a component with dimensions smaller than that of a cell would be needed for proper detection. Therefore smaller devices capable of achieving high transmission, such as the Ph.C. are preferred to larger optical waveguides.

To characterize influence of different media on photonic crystal spectrum, the first set of simulations was conducted in the absence of cells and compared to those when the cell (d = 7μm) was present. Three media were compared: water (refractive index 1.333), and two blood plasma samples with slightly different refractive indices (1.3515 and 1.3575) [20]. Figure 4, shows effects on the transmission spectrum when a blood cell is present on the Ph.C. surface, as well as a response to a change in the surrounding media. While changes in transmission are observed over the entire spectrum, here attention is focused on a narrow region where maximum transmission is occurring. These regions of maximum transmission are where the influence of cells and media are the strongest and the most evident. The central wavelength of maximum transmission is directly related to the refractive index of the surrounding media. Water, with the lowest refractive index, corresponds to peak transmission at a shorter wavelength, while Plasma 2, the highest refractive index fluid, has a peak transmission at longer wavelength. Furthermore, the central wavelength of maximum transmission is not influenced by presence of the cell on the surface. It only effects transmitted light intensity. Based on that, it is possible to not only detect cell presence or absence, but also independently measure the refractive index of the surrounding media.

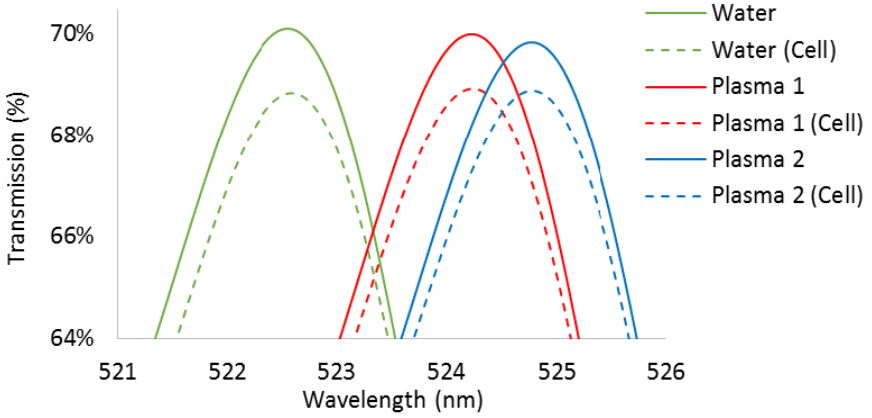

Fig. 4. Peak transmission spectrum for different media, with and without a red blood cell.

Plasma (refractive index 1.3515) was used as the surrounding fluid for the remainder of the study. Once cells were flowing across the surface of the Ph.C., changes in transmission were recorded over the entire spectrum. Figure 5 shows a heat map displaying changes in transmission for a single 7 μm blood cell with respect to both the wavelength of light propagating through the device, as well as the displacement of the cell through the plane. For some wavelengths, e.g. around 524 nm, the blood cell appears to scatter light resulting in overall decrease in transmission, while for other wavelengths, e.g. near 531 nm, the blood cell appears to act as a cladding layer, which actually causes an increase in the transmission through the Ph.C.

After demonstrating of the ability to detect presence of the cell, the next step was to demonstrate that a Ph.C. micro-flow cytometer is capable of replicating the some of the primary functions of lab-scale flow cytometry units. The desired functions are: the ability to

#207945 - $15.00 USD Received 10 Mar 2014; revised 17 Apr 2014; accepted 29 Apr 2014; published 20 May 2014

count cells, to characterize cell shape, as well as determine the size of the cell. Findings from each simulation have been reported at different wavelengths in order to demonstrate the many channels of detection available when using a Ph.C. based device.

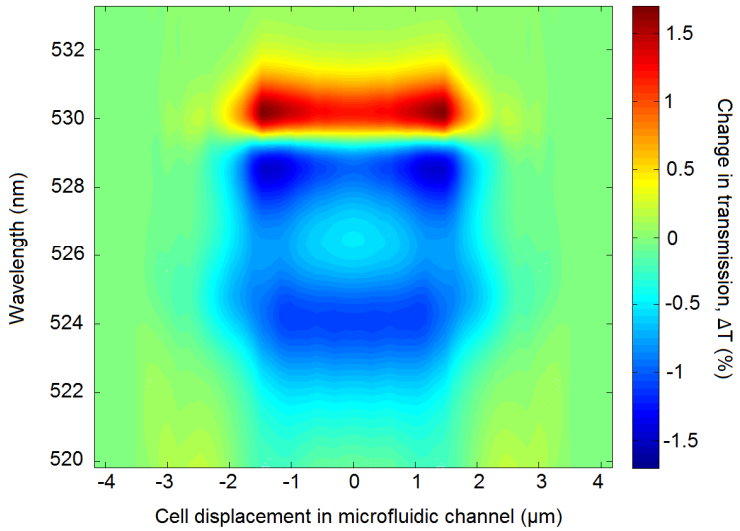

Fig. 5. Heat map displaying difference in transmission caused by cell movement (d = 7μm) for the spectral range 520-533 nm

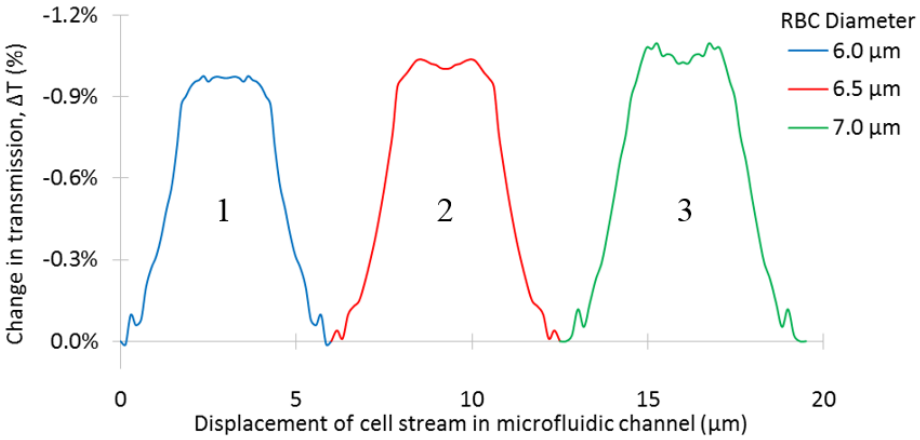

Fig. 6. Transmission change corresponding to three cells flowing in series, detection conducted at λ = 475.8 nm.

In order to demonstrate counting, three blood cells of different diameter (6, 6.5, and 7 μm respectively) were flowed through the device. The simulation was designed such that no space existed between any two cells flowing consecutively in a line through the device, and each sequential blood cell was in direct contact with its neighboring cells as they passed over the Ph.C. surface. Since cells have a natural tendency to sediment, and hydrodynamic focusing can be used in experiments, an assumption was made that cells can always be flowing close to the surface. Changes in transmission (ΔT) were recorded and plotted against the cumulative displacement of the cell stream as it passed through the device. In practice, measurements would be recorded with respect to time, and converted into displacement by

#207945 - $15.00 USD Received 10 Mar 2014; revised 17 Apr 2014; accepted 29 Apr 2014; published 20 May 2014

multiplying time with the velocity of the cell stream. Displacement is used for the plots as it may be easily correlated to the dimensions of the cells. The simulation results are shown in Fig. 6 for a wavelength of 475.8 nm. It can be seen that a characteristic change in transmission was detected as each cell passed through the observation plane. The fact that distinct signals existed for each of the cells demonstrates the capability of such a device to count cells flowing in series. While, the degree to which each cells can be resolved from one another is dependent on the width of Ph.C., as previously shown, this device is able to function at dimensions that are only fractions of a cell diameter.

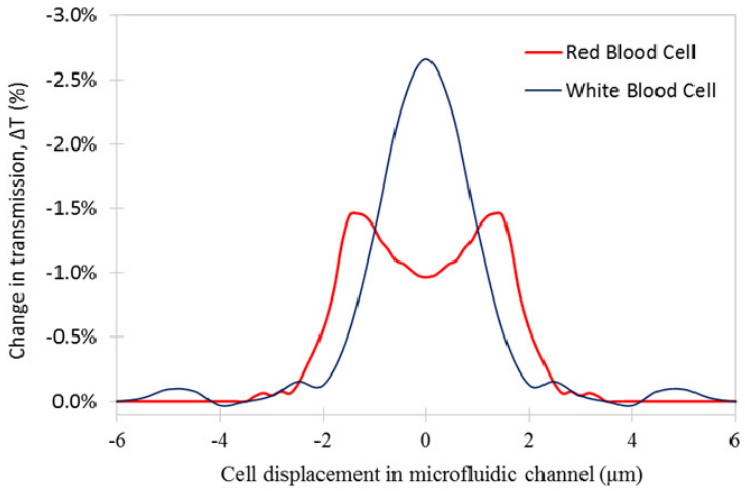

Fig. 7. Change in transmission for different cell types – red blood cell (red) and white blood cell (blue), λ = 528.5 nm.

In Fig. 7, change in transmission due to cell movement is shown for two different shapes. One of them was a 7 μm blood cell, and the other a white blood cell (Refractive index 1.42, diameter 12 μm [23]). Significantly different signal distributions were observed for the two cell types. For the red blood cell, the change in transmission exhibited a symmetric double peaked distribution, while for the white blood cell, the signal was more normally distributed around the center. Comparing signal distribution for the red blood cell to the cross sectional image of the as seen in Fig. 1(a), a connection between the shape of the signal and the physical object can be observed. Thickest portions of the object, such as the center of the cell 'lobes' display the greatest effect on transmission in the Ph.C., while locations of the cell with lower thickness such as the center and edges of the cell have less of an effect overall. Based on that, it can be clearly seen that information regarding cell shape may be extracted with photonic crystal micro-flow cytometry.

#207945 - $15.00 USD Received 10 Mar 2014; revised 17 Apr 2014; accepted 29 Apr 2014; published 20 May 2014

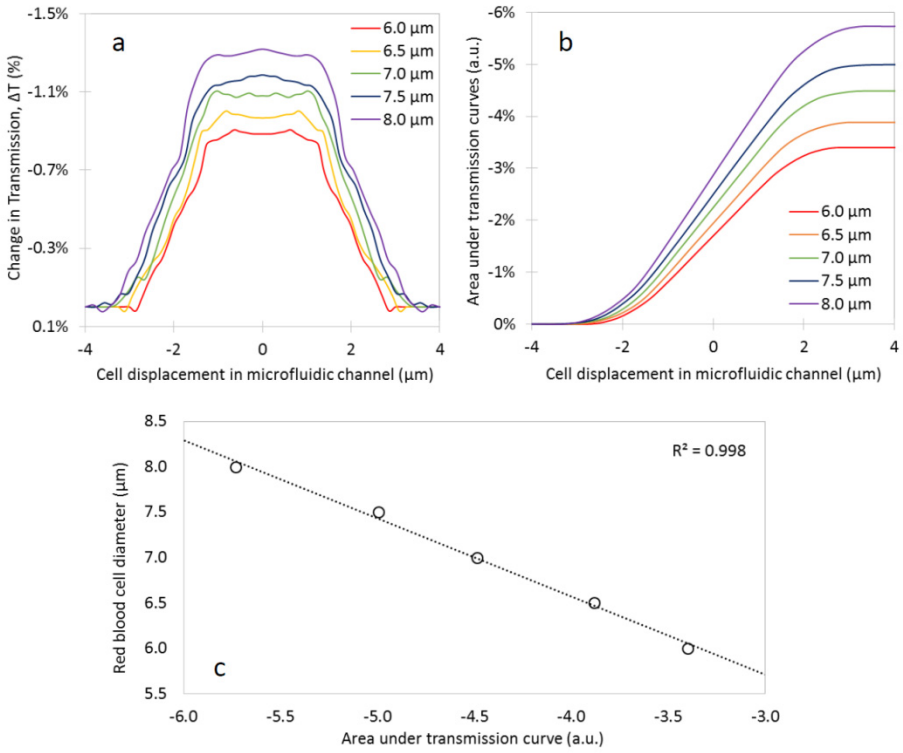

Fig. 8. Change in transmission for cells of different size, λ = 524.1 nm. a) Change of transmission for blood cells of various diameters (6-8 µm) w.r.t. cell displacement in the microfluidic channel. b) Numerical integration of area under transmission change curves. c) Correlation between blood cell diameter and the area under the transmission change curves.

Finally, a correlation between red blood cell size and change in transmission was required to achieve a working model for a functional micro-flow cytometer. In order to accomplish this, blood cells ranging from 6 to 8 µm in diameter were analyzed with the proposed device. Figure 8(a) represents the change in transmission ΔT measured at a wavelength of 524.1 nm for each of the cells in relation to their displacement through the observation plane δy. It can be noticed that as blood cell diameter increased the overall area under the corresponding transmission signal increased as well. The area under each transmission curve was determined through numerical integration and plotted as a function of displacement δy in Fig. 8(b). Results for the areas under each curve were then plotted against their corresponding blood cell diameter (Fig. 8(c)). Based on the coefficient of determination R^2, there is a strong correlation between the transmission area and the red blood cell diameter.

4. Conclusions

A novel design for a micro-flow cytometer using 1-D photonic crystals has been demonstrated. The device was modeled using finite difference time domain (FDTD) simulations. It was shown that the device is capable of not only detecting counting cells, but is also able to provide information regarding cell shape, as well as its size. Different wavelengths can be simultaneously used for multiple information channels. Altogether, this photonic crystal micro-flow cytometry system achieves several functions similar to the functions of large scale, traditional flow cytometry units, however on a scale small enough that the device may be integrated onto a chip.

#207945 - $15.00 USD Received 10 Mar 2014; revised 17 Apr 2014; accepted 29 Apr 2014; published 20 May 2014